Article

Localised Web Bearing Behaviour of Cold-Formed Austenitic Stainless-Steel Channels: Review of Design Rules and New Insight under Interior Loading

Amir M. Yousefi [1,*], Bijan Samali [1] and Yang Yu [2]

1   School of Engineering, Design and Built Environment, Western Sydney University, Sydney, NSW 2751, Australia; b.samali@westernsydney.edu.au
2   Centre for Infrastructure Engineering and Safety, School of Civil and Environmental Engineering, University of New South Wales (UNSW), Sydney, NSW 2052, Australia; yang.yu12@unsw.edu.au
*   Correspondence: amir.yousefi@westernsydney.edu.au

Abstract: Stainless steels are modern high-performance construction materials exhibiting excellent corrosion resistance, recyclability, ductility, and durability which make them appealing to use in the construction industry. However, when used as structural sections, they are subjected to localised failure in the web. This study aims to examine the structural behaviour of cold-formed low-carbon content standard austenitic 304L and 316L stainless steel channels under localised interior bearing loads. The results of 21 tests on unlipped channels with different cross-section sizes and thicknesses are presented. A nonlinear quasi-static Finite Element (FE) model is then developed. The FE model is validated against experimental test results and demonstrated good agreement in terms of bearing strength and failure modes. In addition, the experimental and FE results are used to compare the results against the results predicted in accordance with the American specification SEI/ASCE 8:2002 and European Standard EN 1993-1-4:2006. It is found that the current design equations are unreliable and too unconservative to use for cold-formed austenitic stainless steel unlipped channels, especially when compared to SEI/ASCE 8:2002, as much as 41%.

Keywords: austenitic stainless steel; cold-formed steel; experimental investigation; finite element modelling; web-bearing strength

1. Introduction

The high-strength Stainless steels are used in construction due to their high corrosion resistance and strength making them appealing to use as load-bearing structural components in the building industry [1,2]. The three primary material grades of stainless steels are known as ferritic, austenitic, and duplex. Out of three stainless steel grades, austenitic provides great formability, heat resistance and non-magnetic properties. The nickel content in austenitic ranged between 8% to 11%, while chromium content is between 17% to 18% offering great corrosion resistance. Such unique benefits of austenitic stainless steel made its widespread use in structural applications [3]. The low-carbon content standard austenitic 304L and 316L stainless steels are one of the most extensively used in the modern construction industry because of their complete austenitic structure. This is particularly applied to components with low magnetic permeability requirements [4,5]. Despite such advantages, no test results have been reported in the current literature for austenitic 304L and 316L stainless steel unlipped channel sections under localised interior bearing loads.

In the literature, Korvink et al. [6,7] reported a series of web earing test results on lipped stainless-steel channels under one-flange loading. However, such tests were only carried out on different loading cases, and thus, the influences of interior localised loading were not included. Li and Young [8] carried out a total of 37 tests on cold-formed ferritic stainless steel hollow members under localised web-bearing loads. From this study, improved design

rules for these hollow sections were proposed. In another study, Cai and Young [9,10] tested cold-formed duplex stainless steel hollow sections under different localised web-bearing loads. From more recent studies by Yousefi et al. [11,12], new Finite Element models and design equations were developed for ferritic and austenitic stainless-steel channels under web-bearing loads. However, ferritic stainless steel unlipped channels subject to interior loading conditions were not covered. Such channels are used as load-bearing components on solid foundations. In previous research studies [13–16], web-bearing capacity reduction factor equations have been proposed for cold-formed ferritic stainless-steel channels having centred and offset holes in the web. However, the channels were with web holes and manufactured with ferritic stainless steel as well as tested under different loading cases, namely two flange loadings. Similarly, Yousefi et al. [17–20] performed numerical investigations on the web-bearing capacity of stainless steel-lipped channels having holes in the web and proposed new web-bearing capacity reduction factor equations. However, the proposed equations were recommended only for lipped channels and no experimental results were conducted to confirm the accuracy of the results.

Currently, no test results have been reported on austenitic stainless steel unlipped channels subject to web bearing under interior localised loading. In a recent study, a series of experimental tests were carried out on unlipped ferritic stainless steel channels having holes in the web [21]. In other studies [22,23], perforated ferritic stainless steel unlipped channels were tested, and capacity reduction factor equations were recommended from both tests and numerical investigations. However, these equations are proposed for channels having holes in the web and not for channels without web holes under interior localized loading. For the first time, this issue is addressed herein. In regard to design rules, Australian/New Zealand standard AS/NZS 4673 [24], American standard SEI/ASCE-8 [25], and European code EN 1993-1-4 [26] provide design rules for the design of cold-formed stainless-steel components. Australian/New Zealand standard AS/NZS 4673 [24] adopted from American standard SEI/ASCE-8 [25] and European code EN 1993-1-4 [26] refers to EN 1993-1-3 [27] for carbon steel. However, up to date, no stainless-steel code offers a design equation for stainless steel channels subject to web bearing under interior localised loading where used as load-bearing components on a solid foundation. This research aims to address this gap of knowledge.

In this research, the web-bearing capacity of cold-formed low-carbon content standard austenitic 304L and 316L stainless steel channels under localised interior bearing loads is experimentally and analytically investigated. In total, 21 test results for channels with different cross-section heights and thicknesses are reported. Furthermore, considering the material nonlinearity of stainless steels, quasi-static Finite Element (FE) models are developed using ABAQUS 6.25 [28]. Subsequently, the developed FE model is verified against test results carried out from this study and shows a good match in terms of web-bearing capacity and mode of failure. In addition, to assess the accuracy and validity of current design equations, the test and FE results from this study are compared against the web-bearing capacities determined from the current stainless steel design codes [25,26]. Finally, it is noted that the available design equations are too unconservative and unreliable to use for cold-formed austenitic stainless-steel channels under localised interior bearing loads, especially when compared to SEI/ASCE 8 [25], as much as 41%.

2. Web Bearing Capacity Design of Cold-Formed Austenitic Stainless-Steel Channels

As noted previously, Australian/New Zealand standard AS/NZS 4673 [24], American standard SEI/ASCE-8 [25], and European code EN 1993-1-4 [26] provide design rules for the design of cold-formed stainless-steel components. Australian/New Zealand standard AS/NZS 4673 [24] adopted from American standard SEI/ASCE-8 [25] and European code EN 1993-1-4 [26] refers to EN 1993-1-3 [27] for carbon steel. However, up to date, no stainless-steel code offers a design equation for stainless steel channels subject to web bearing under interior localised loading. This research aims to address this gap of knowledge. In this paper, the web-bearing capacity of cold-formed austenitic stainless steel

unlipped channels subject to localised web-bearing interior loading is described. The results of 21 tests on unlipped channels with various cross-section sizes and thicknesses are presented. To examine the accuracy and suitability of current design equations, the laboratory and numerical results were compared with the results predicted from the American specification SEI/ASCE 8:2002 [29] and European Standard EN 1993-1-4:2006 [30]. A summary of design guidelines has been summarised in the following sections.

2.1. ASCE Specification

According to SEI/ASCE-8, the nominal web crippling strength (P_n) for cold-formed unlipped channels is determined using the following Equations (1)–(4). The SEI/ASCE-8 provides a set of equations to calculate the web bearing strength (P_{ASCE}) of unlipped channels under concentrated load or reaction for one solid web connecting the top and bottom flanges without any web openings.

For unlipped channels under IOF loading:

$$P_n = t^2 C_1 C_2 C_\theta \left(538 - 0.74\frac{h}{t} \right) \times \left(1 + 0.007\frac{N}{t} \right) \times C_t \tag{1}$$

For unlipped channels under EOF loading:

$$P_n = t^2 C_3 C_4 C_\theta \left(217 - 0.28\frac{h}{t} \right) \times \left(1 + 0.01\frac{N}{t} \right) \times C_t \tag{2}$$

For unlipped channels under ITF loading:

$$P_n = t^2 C_1 C_2 C_\theta \left(771 - 2.26\frac{h}{t} \right) \times \left(1 + 0.0013\frac{N}{t} \right) \times C_t \tag{3}$$

For unlipped channels under ETF loading:

$$P_n = t^2 C_3 C_4 C_\theta \left(224 - 0.57\frac{h}{t} \right) \times \left(1 + 0.01\frac{N}{t} \right) \times C_t \tag{4}$$

where:

IOF is Interior-One-Flange,
EOF is End-One-Flange,
ITF is Interior-Two-Flange,
ETF is End-Two-Flange,
h is the depth of the flat portion of the web measured along the plane of the web,
P_n is the nominal localised bearing strength for unlipped channels,
R is the inside bend radius,
t is the web thickness,
N is the actual length of the bearing.

In the formulas:

$$C_t = 6.9 \text{ for SI Units}$$

$$C_\theta = 0.7 - 0.3\left(\frac{\theta}{90} \right)^2$$

$$\text{If } F_y/(91.5\ C_t) \ \le\ 1.0, \text{ then } C_1 = (1.22 - 0.22k)k$$

$$\text{If } F_y/(91.5\ C_t) \ >\ 1.0, \text{ then } C_1 = 1.69$$

$$C_2 = (1.06 - 0.06\frac{R}{t}) \le 1.0$$

$$C_3 = (1.33 - 0.33k)k \qquad \text{when} \qquad F_y / 66.5\, C_t \ \le\ 1.0$$

$$C_3 = 1.34 \qquad \text{when} \qquad F_y / 66.5\, C_t \ >\ 1.0$$

$$C_4 = (1.15 - 0.15\, R/t) \le 1.0 \text{ but not less than } 0.50$$

$$k = \frac{F_y}{33 C_t}$$

$$m = t/0.075 \text{ for SI Units}$$

The above equations are applied within the following limits:

$$N/t \le 210 \text{ and } N/h \le 3.5$$

$$R/t \le 6 \text{ for beams.}$$

2.2. European Code

In this code, a set of equations has been provided to determine the web-bearing capacity of unlipped channels under localised loading. Such equations are used to avoid crippling, crushing or buckling in a web subject to a support reaction or other local concentrated transverse force applied through the flanges.

In the following, the design equations for single unstiffened webs are given.

The local transverse resistance of the web ($R_{w,Rd}$) for a cross-section with a single unstiffened web, is calculated from Equations (5)–(10) on a condition that the cross-section meets the criteria below:

$$h_w / t \le 200$$

$$r / t \le 6$$

$$45° \le \varphi \le 90°$$

where:

h_w is the web height between the midlines of the flanges;
r is the internal radius of the corners;
θ is the angle of the web relative to the flanges (degrees).

From the EN 1993-1-3 standard, the local transverse resistance $R_{w,Rd}$ of a single web under interior-one-flange (IOF) loading can be calculated from:

For $c > 1.5 h_w$ clear from a free end and for a cross-section with unstiffened flanges:
If $S_S / t \le 60$:

$$R_{w,Rd} = \frac{k_3 k_4 k_5 \left[14.7 - \frac{h_w/t}{49.5}\right] \left[1 + 0.007 \frac{S_S}{t}\right] t^2 f_{yb}}{\gamma_{M1}} \tag{5}$$

If $S_S / t \ge 60$:

$$R_{w,Rd} = \frac{k_3 k_4 k_5 \left[14.7 - \frac{h_w/t}{49.5}\right] \left[0.75 + 0.011 \frac{S_s}{t}\right] t^2 f_{yb}}{\gamma_{M1}} \tag{6}$$

The local transverse resistance $R_{w,Rd}$ of a single web under end-one-flange (EOF) loading can be calculated from:

For $c \le 1.5 h_w$ clear from a free end and for a cross-section with unstiffened flanges:

If $S_S/t \leq 60$:

$$R_{w,Rd} = \frac{k_1 k_2 k_3 \left[5.92 - \frac{h_w/t}{132}\right]\left[1 + 0.01\frac{S_S}{t}\right] t^2 f_{yb}}{\gamma_{M1}} \qquad (7)$$

If $S_S/t \geq 60$:

$$R_{w,Rd} = \frac{k_1 k_2 k_3 \left[5.92 - \frac{h_w/t}{132}\right]\left[0.71 + 0.015\frac{S_s}{t}\right] t^2 f_{yb}}{\gamma_{M1}} \qquad (8)$$

The local transverse resistance $R_{w,Rd}$ of a single web under interior-two-flange (ITF) loading can be calculated from:

For $c > 1.5h_w$ clear from a free end and for a cross-section with unstiffened flanges:

$$R_{w,Rd} = \frac{k_3 k_4 k_5 \left[21.0 - \frac{h_w/t}{16.3}\right]\left[1 + 0.0013\frac{S_s}{t}\right] t^2 f_{yb}}{\gamma_{M1}} \qquad (9)$$

The local transverse resistance $R_{w,Rd}$ of a single web under end-two-flange (ETF) loading can be calculated from:

For $c \leq 1.5h_w$ clear from a free end and for a cross-section with unstiffened flanges:

$$R_{w,Rd} = \frac{k_1 k_2 k_3 \left[6.66 - \frac{h_w/t}{64}\right]\left[1 + 0.01\frac{S_s}{t}\right] t^2 f_{yb}}{\gamma_{M1}} \qquad (10)$$

where:

c is the distance from loading to the closest end of the beam;
S_s is the nominal length of stiff bearing;
f_{yb} is the yield strength of steel;
γ_{M1} is the partial safety factor,
$\gamma_{M1} = 1.00$.

The values of the coefficients k_1 to k_5 should be determined as follows:

$$k_1 = (1.33 - 0.33k)$$

$$k_2 = (1.15 - 0.15\,r/t), \text{ but } k \geq 0.5 \text{ and } k \leq 1.0\text{-change this to } K_2$$

$$k_3 = 0.7 + 0.3\left(\varphi/90\right)^2$$

$$k_4 = (1.22 - 0.22k)$$

$$k_5 = (1.06 - 0.06\,r/t) \text{ but } k_5 \leq 1.0$$

$$k = f_{yb}/228 \ (f_{yb} \text{ in N/mm}^2)$$

2.3. American Iron and Steel Institute Specification

According to this specification [31], known as the North American Specification (NAS), the following Equation (11) can be used in order to determine the nominal web-bearing capacity (P_{NAS}) of cold-formed steel unlipped and lipped channels subjected to localised loading:

$$P_{NAS} = Ct^2 F_y sin\theta \left(1 - C_R\sqrt{\frac{R}{t}}\right)\left(1 - C_N\sqrt{\frac{N}{t}}\right)\left(1 - C_h\sqrt{\frac{h}{t}}\right) \qquad (11)$$

In the above equation, C is the coefficient, C_N is the bearing length coefficient, C_R is the inside corner radius coefficient, C_h is the slenderness coefficient, F_y is the design strength, h is the flat dimension of the web measured in the plane of the web, N is the bearing length, R is the inside bend radius, t is the web thickness, θ is the angle between the plane of the web and the plane of the bearing surface.

3. Experimental Investigation

The testing programme comprised 21 channels, tested using a Universal Instron Testing Machine. The tested channel sections had various web heights ranging from 100 mm to 250 mm, where the depth of the flat portion of the web over web thickness (h/t) ranged from 60.9 to 82.6 in the experimental programme. Considering the guideline of AISI S100 [31], the length of tested channels (L) was threefold the web height plus the length of the top bearing plate. The channels were tested as a single web channel, where the details and dimensions measured in the lab have been presented in Table 1. Nomenclature of the tested channels is shown in the Figure 1a.

Table 1. Measured channel specimen details and laboratory ultimate loads for channels under localised Interior Loading (IL).

Channel	Plate Length N (mm)	Web Height d (mm)	Flange Width b_f (mm)	Web Thickness t (mm)	Fillet Radius r (mm)	Channel Length L (mm)	Experimental Ultimate Force F_{Exp} (kN)
C100×50-t1.50-N50	50	100.24	50.32	1.48	5.00	350.21	5.23
C100×50-t1.50-N75	75	100.73	50.74	1.49	5.00	373.83	5.49
C100×50-t1.50-N100	100	100.63	50.95	1.48	5.00	398.67	5.72
C125×50-t1.50-N50	50	123.91	49.89	1.49	5.00	424.00	5.43
C125×50-t1.50-N75	75	125.60	49.75	1.50	5.00	449.67	5.56
C125×50-t1.50-N100	100	125.44	49.90	1.50	5.00	475.67	5.81
C150×60-t2.0-N50	50	150.84	59.62	2.00	5.50	501.00	10.45
C150×60-t2.0-N75	75	149.62	60.71	2.00	5.50	526.00	10.64
C150×60-t2.0-N100	100	149.17	60.52	1.98	5.50	550.33	10.94
C175×60-t2.0-N50	50	175.40	60.86	1.99	5.50	576.50	10.28
C175×60-t2.0-N75	75	175.28	60.84	2.00	5.50	599.17	10.69
C175×60-t2.0-N100	100	174.15	60.27	2.00	5.50	626.17	10.97
C200×75-t3.0-N50	50	201.50	74.64	3.00	6.00	650.83	26.04
C200×75-t3.0-N75	75	201.45	74.49	2.99	6.00	674.33	26.50
C200×75-t3.0-N100	100	201.58	74.17	3.00	6.00	699.00	27.10
C225×75-t3.0-N50	50	225.50	74.54	3.00	6.00	725.50	26.45
C225×75-t3.0-N75	75	226.00	74.27	2.99	6.00	749.33	27.08
C225×75-t3.0-N100	100	225.50	74.73	2.98	6.00	775.33	26.09
C250×75-t3.0-N50	50	249.75	74.35	2.99	6.00	726.00	24.01
C250×75-t3.0-N75	75	250.50	74.68	2.99	6.00	749.33	24.39
C250×75-t3.0-N100	100	249.75	74.46	2.99	6.00	775.50	23.05

For simplicity in identifying the test channels, specimen labelling comprised of the channel thickness, dimensions, and top loading plate length. The channel labelled as "200×75-t3.0-N50" is clarified as follows. The first part of the labelling as "200 × 75" implies the nominal height of the channel and flange width in units of millimetres, while "t3.0" indicates the thickness of the web being equal to 3.0 mm. The annotation "N" denotes the length of the top load-bearing plate.

As shown in Figure 1b, the channel specimens were tested subject to concentrated transverse localised force, namely Interior Loading (IL). The channels were tested considering AISI S100 [31]. The vertical force is applied to the mid-length of channels on top channel flanges using a high-strength steel plate. Steel half rounds were placed on top of the steel loading plate at mid-length of the channel specimen considering vertical alignment with line of forces. Using the Instron Universal Testing Machine, a linear constant load with a load rate of 0.5 mm/min was applied. The testing configuration for channel specimens subject to Interior Loading (IL) is shown in Figure 1b. A series of 9 tensile coupon tests were conducted to determine the mechanical properties of the channel specimens. Figure 2

shows the tensile coupon test set-up and stress-strain curve for channels with 3 mm thickness fabricated with G304L stainless steel, while Table 2 provides the material properties of the tested tensile coupons. The corresponding hot-rolled steel mechanical properties are found in Rezvani et al. [32].
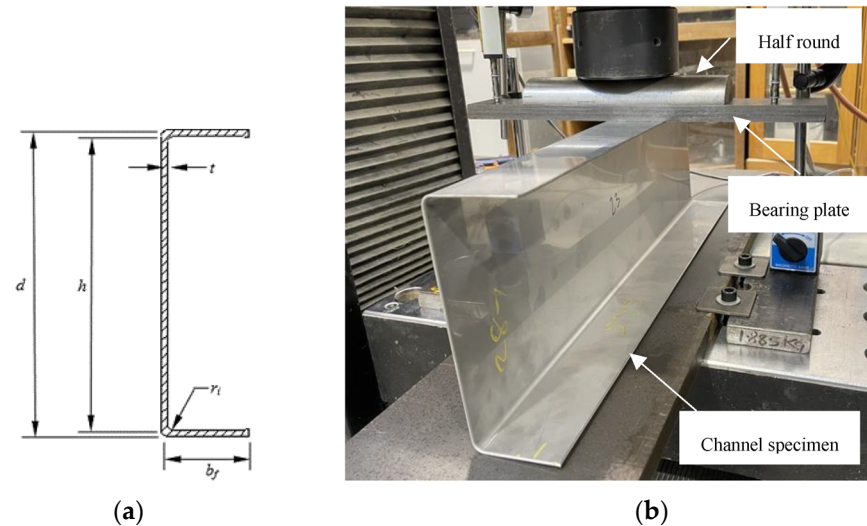

(**a**)   (**b**)

Figure 1. Stainless steel channels test. (**a**) Symbols definition; (**b**) Testing set-up for channels under IL loading condition.
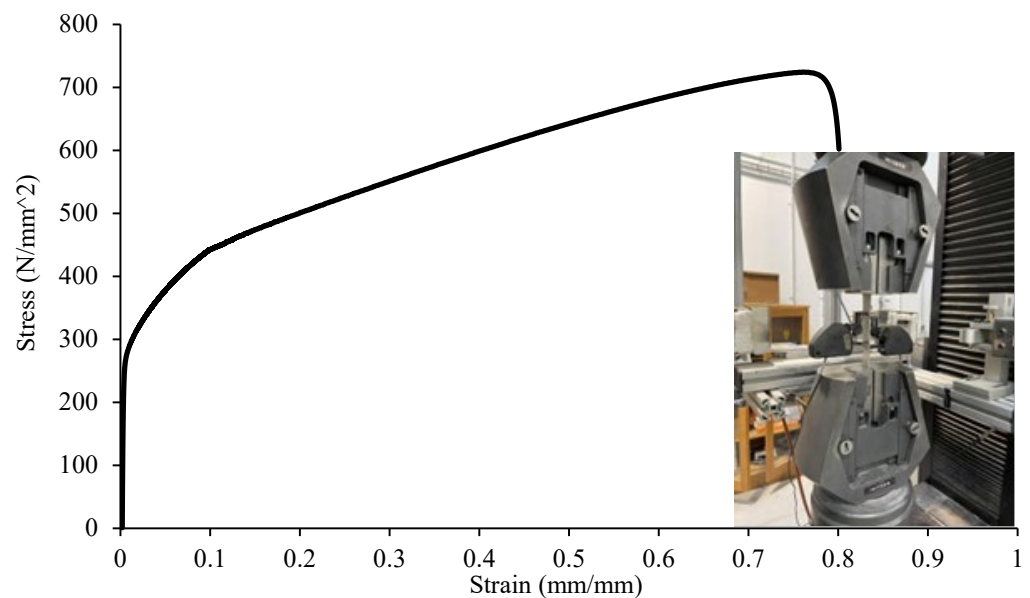

Figure 2. Tensile coupon test [11].

As previously mentioned, the testing programme comprised of a series of 21 channels with different channel sizes and thicknesses subjected to localised interior bearing loading. The experimental ultimate bearing capacities for single web channels, denoted as F_{EXP}, are given in Table 1. The typical mode of failures for the tested are depicted in Figure 3a,b. The laboratory test results are given in Table 1. Load-displacement curves obtained from tested channels labelled as C100×50-t1.50-N100, C150×60-t2.0-N100, C200×75-t3.0-N75, and C250×75-t3.0-N50 under Localised Interior Loading are shown in Figure 4 to provide more information.

Table 2. Material properties determined from tensile tests.

Tensile Coupon	Base Metal Coupon Thickness (mm)	Gauge Width (mm)	Gauge Length (mm)	Elastic Modulus (MPa)	Tensile Yield Strength ($\sigma_{0.2}$) (MPa)	Ultimate Tensile Strength (σ_u) (MPa)
1.5 mm thickness	1.48	20.0	50.0	200.0	264.0	594.0
G316L-EN 1.4404	1.47	20.0	50.0	198.0	252.0	608.0
	1.49	20.0	50.0	197.0	261.0	595.0
	---	---	---		259.0	599.0
2.0 mm thickness	1.97	20.0	50.0	198.0	280.0	695.0
G304L-EN 1.4307	1.99	20.0	50.0	200.0	293.0	709.0
	1.98	20.0	50.0	197.0	285.0	705.0
	---	---	---		286.0	703.0
3.0 mm thickness	2.98	20.0	50.0	197.0	291.0	730.0
G304L-EN 1.4307	2.96	20.0	50.0	200.0	289.0	711.0
	2.97	20.0	50.0	198.0	293.0	731.0
	---	---	---		290.0	724.0

(a)

(c)

Reference point applying load in y direction
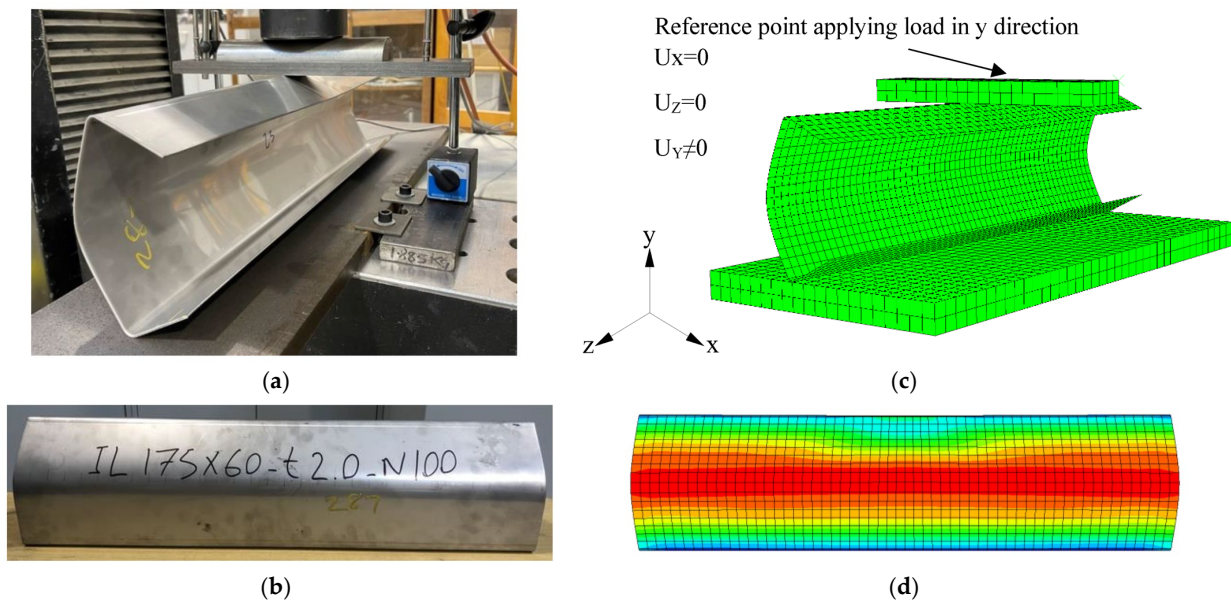Ux=0
Uz=0
Uy≠0

(b)

(d)

Figure 3. Experimental and Finite Element failure modes of channels. (**a**) Experimental 3D view; (**b**) Experimental front view; (**c**) Finite element 3D view; (**d**) Finite element front view [11].
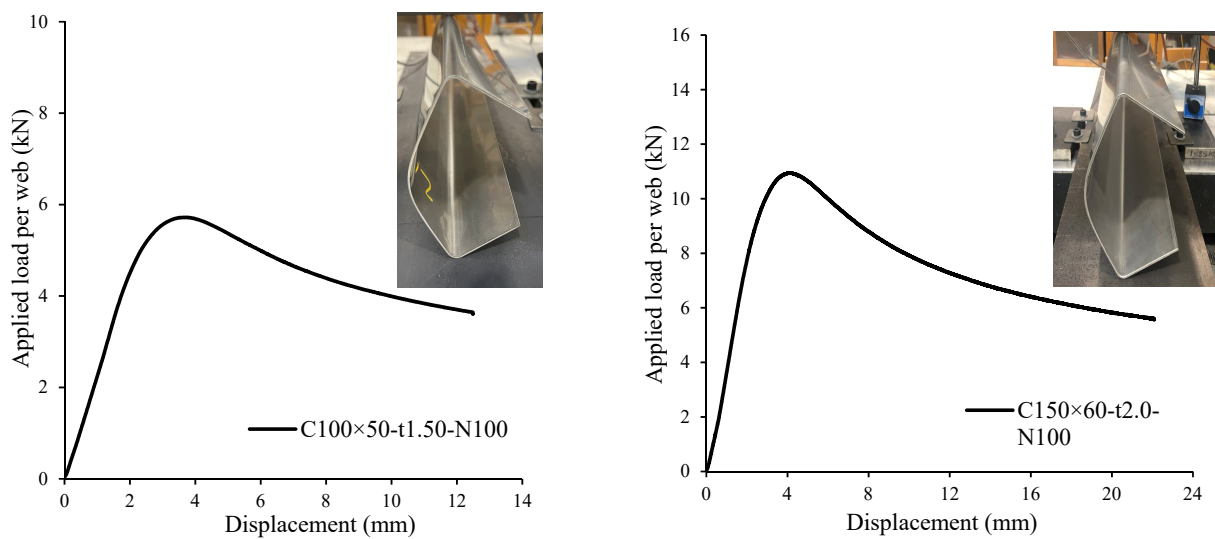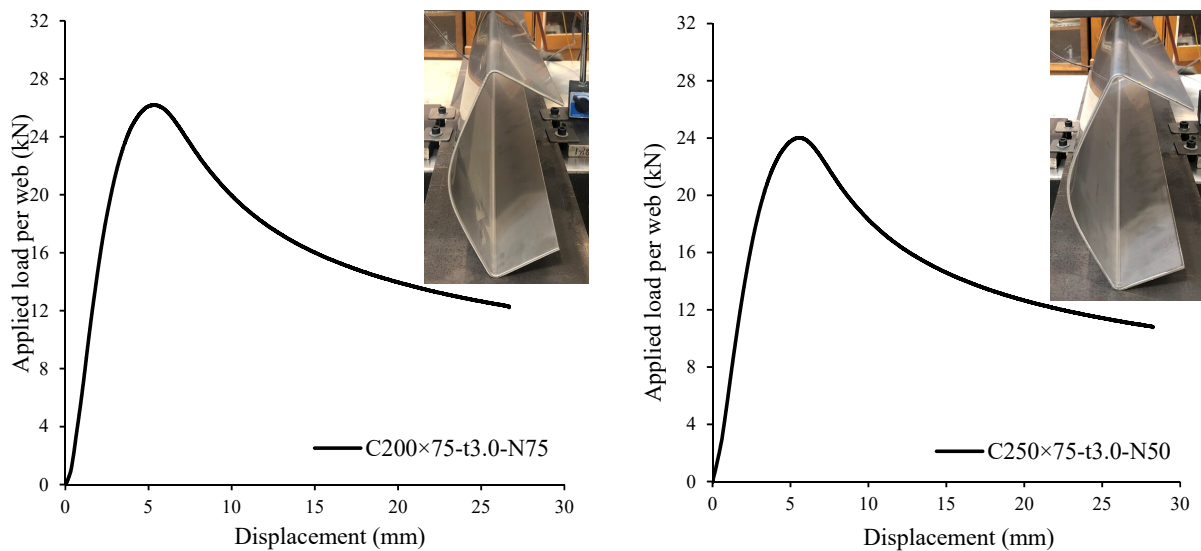

Figure 4. *Cont*.

Figure 4. Experimental web deformation curves for channels with various cross-section sizes [11].

4. Numerical Investigation

To model the test set-up including channel sections and top load-bearing plate, the multi-application finite element (FE) software programme ABAQUS 6.25 [28] was utilised in the numerical investigation. The cross-sectional sizes and details of the channel models were based on measurements conducted in the lab and the nonlinearity of the material was considered in the numerical investigations. In addition, consistent with recent research by Mohammadjani et al. [33] and Natário et al. [34], where explicit dynamic analysis was considered, in this study, a quasi-static procedure was adopted based on implicit integration analysis. This analysis type is found advantageous considering the complex nonlinearity material behaviour of cold-formed stainless steel beams. The finite element modelling details are presented below. More detailed modelling has been described by the authors [35–37] while further modelling techniques are described in recent studies [38–40].

From the ABAQUS 6.25 [28] library, S4R thin-shell elements representing channel models were used for modelling. This element is appropriate for applications with complex buckling behaviour such as thin-walled sections. Accordingly, a general purpose C3D8R element taking into account strain and plasticity applications and considering large deformation effects was used to model the top load-bearing plate. Using the following Equations (1) and (2) obtained from the ABAQUS 6.25 manual [28], the engineering stress-strain curve from tensile coupon tests from this study was converted to a true stress-strain curve and applied to the models. Figure 5 demonstrates the finite element (FE) models for the channel models having different bearing stages subjected to bearing failure under interior loading conditions. In addition, from this figure, the typical FE meshes for channel models and top load-bearing plates have been illustrated. The mesh sizes of 5 × 5 mm and 8 × 8 mm were used for channel models and top load-bearing plates, respectively, wherein the conjunction of the web and flanges, finer mesh size was utilised.
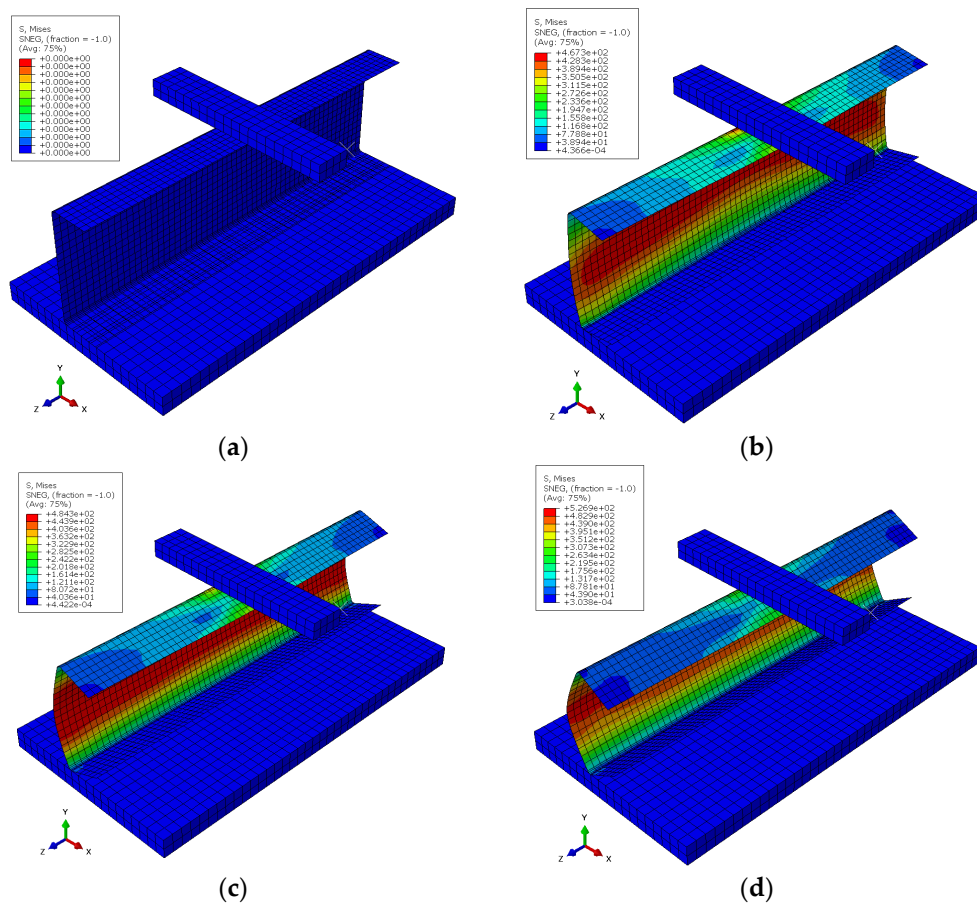
Figure 5. Deformation under progressive loading of the C150×60 under IL loading. (**a**) Initial; (**b**) Before peak; (**c**) Peak; (**d**) Post-peak [11].

From the ABAQUS 6.25 manual [28], the engineering stress-strain curve from tensile coupon tests from this study was converted to a true stress-strain curve and applied to the models. The equations for this conversion have been presented below:

$$\sigma_{true} = \sigma(1 + \varepsilon) \tag{12}$$

$$\varepsilon_{true(pl)} = ln(1 + \varepsilon) - \frac{\sigma_{true}}{E} \tag{13}$$

In which σ_{true} is the true stress, $\varepsilon_{true(pl)}$ is the logarithmic plastic strain, E is the modulus of Young, and σ is the engineering stress, while ε is the engineering strain.

To verify the suitability and accuracy of the FE models, the results from laboratory tests were compared against the results obtained from FE modelling. This ultimate bearing capacity comparison from lab tests and numerical modelling for single web channels (F_{EXP} and F_{FEA}) is summarised in Table 3. The results showed a very good match achieved between the results from the tests and FE models. Looking at the same table in more detail, the average ratio of the test results over FE results (F_{EXP}/F_{FEA}) is 0.99, with a coefficient of variation of 0.01. The channels labelled as C125×50-t1.50-N100 and C250×75-t3.0-N100 have shown only 3% differences between the results from the tests and FE models with other channels have shown less than 3% errors.

Table 3. Experimental and FE ultimate loads for channels under IL loading.

Channel	Web Height Ratio (h/t)	Plate Length Ratio (N/t)	Fillet Radius Ratio (r/t)	Experimental Ultimate Load F_{Exp} (kN)	Finite Element Ultimate Load F_{FEA} (kN)	Comparison F_{EXP}/F_{FEA}
C100×50-t1.50-N50	60.97	33.78	3.38	5.23	5.31	0.98
C100×50-t1.50-N75	60.89	50.34	3.36	5.49	5.61	0.98
C100×50-t1.50-N100	61.24	67.57	3.38	5.72	5.83	0.98
C125×50-t1.50-N50	76.45	33.56	3.36	5.43	5.56	0.98
C125×50-t1.50-N75	77.07	50.00	3.33	5.56	5.68	0.98
C125×50-t1.50-N100	76.96	66.67	3.33	5.81	5.98	0.97
C150×60-t2.0-N50	69.92	25.00	2.75	10.45	10.58	0.99
C150×60-t2.0-N75	69.31	37.50	2.75	10.64	10.72	0.99
C150×60-t2.0-N100	69.78	50.51	2.78	10.94	10.99	1.00
C175×60-t2.0-N50	82.61	25.13	2.76	10.28	10.36	0.99
C175×60-t2.0-N75	82.14	37.50	2.75	10.69	10.74	1.00
C175×60-t2.0-N100	81.58	50.00	2.75	10.97	11.05	0.99
C200×75-t3.0-N50	63.17	16.67	2.00	26.04	26.12	1.00
C200×75-t3.0-N75	63.36	25.08	2.01	26.50	26.63	1.00
C200×75-t3.0-N100	63.19	33.33	2.00	27.10	27.19	1.00
C225×75-t3.0-N50	71.17	16.67	2.00	26.45	26.31	1.01
C225×75-t3.0-N75	71.57	25.08	2.01	27.08	26.90	1.01
C225×75-t3.0-N100	71.64	33.56	2.01	26.09	25.94	1.01
C250×75-t3.0-N50	79.52	16.72	2.01	24.01	23.61	1.02
C250×75-t3.0-N75	79.77	25.08	2.01	24.39	24.11	1.01
C250×75-t3.0-N100	79.52	33.44	2.01	23.05	22.41	1.03
Mean						0.99
COV						0.01
Reliability						2.61

In addition, the mode of failure comparison from a tested channel specimen against a simulated FE model is shown in Figure 3. This confirms a good web-bearing mode of failure prediction between the developed FE model and lab tests. Furthermore, load-displacement comparison for C175×60-t2.0-N50 under IL loading is also presented in Figure 6. It can be seen that, developed FE models are in very good agreement with laboratory test results and are used to evaluate the suitability of available current design equations.
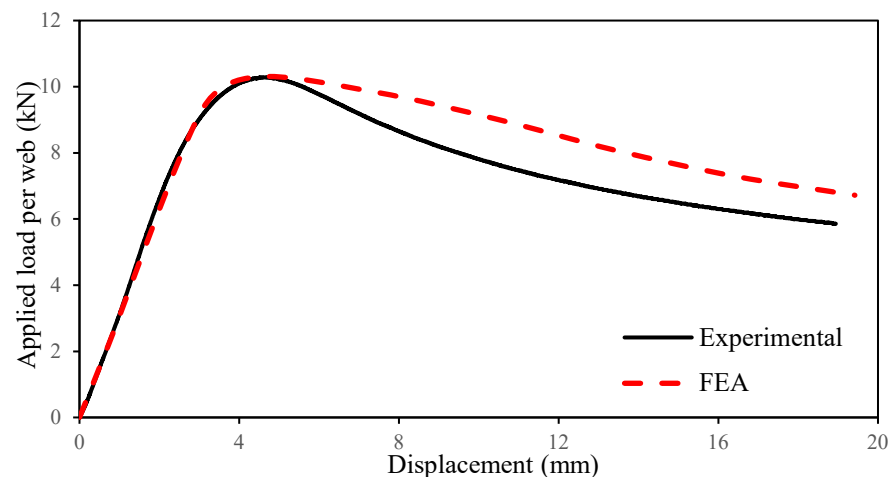
Figure 6. Load-displacement comparison for C175×60-t2.0-N50 under IL loading [11].

5. Design Comparisons of Web Bearing Capacity with Current Design Codes

As stated previously, despite recent advancements in cold-formed stainless steel [41–52], particularly recent research studies on web-bearing capacity [53–58], available cold-formed stainless steel design regulations [25,26] provide no web-bearing capacity equation to address the design of cold-formed austenitic stainless steel channels under localised interior bearing loading. Australian/New Zealand standard AS/NZS 4673 [24],

American standard SEI/ASCE-8 [25], and European code EN 1993-1-4 [26] provide design rules for the design of cold-formed stainless steel components. Australian/New Zealand standard AS/NZS 4673 [24] adopted from American standard SEI/ASCE-8 [25] and European code EN 1993-1-4 [26] refers to EN 1993-1-3 [27] for carbon steel. To assess the accuracy and validity of the current design equations, the web-bearing capacities determined from both laboratory and FE results were compared with the capacities predicted from design codes.

Table 4 presents the web-bearing capacities obtained from laboratory tests for various channel dimensions as well as the capacities predicted from SEI/ASCE-8 [25], and EN 1993-1-4 [26]. Comparing the comparison ratios for both design codes, It is clear that capacities from laboratory tests over the capacities determined from SEI/ASCE-8 [25] averaged equal to 0.59 having a coefficient of variation of 0.04. This implies that the aforementioned design code is overly unconservative as much as 41% to predict web bearing capacities. Comparing the results from laboratory tests over the capacities determined from EN 1993-1-4 [26] averaged equal to 0.66 having a coefficient of variation of 0.03. This shows that this design code is too unconservative as much as 34% to predict web-bearing capacities.

Table 4. Comparison of laboratory web bearing capacities with design codes under IL loading scenario.

Channel	Failure Load	Single Web Bearing Capacity		Comparison	
	F_F (kN)	F_{ASCE} (kN)	F_{EURO} (kN)	F_F/F_{ASCE}	F_F/F_{EURO}
C100×50-t1.50-N50	5.23	9.29	8.32	0.56	0.63
C100×50-t1.50-N75	5.49	9.63	8.62	0.57	0.64
C100×50-t1.50-N100	5.72	9.67	8.66	0.59	0.66
C125×50-t1.50-N50	5.43	8.90	7.97	0.61	0.68
C125×50-t1.50-N75	5.56	9.20	8.24	0.60	0.67
C125×50-t1.50-N100	5.81	9.39	8.41	0.62	0.69
C150×60-t2.0-N50	10.45	18.29	16.39	0.57	0.64
C150×60-t2.0-N75	10.64	18.62	16.68	0.57	0.64
C150×60-t2.0-N100	10.94	18.47	16.55	0.59	0.66
C175×60-t2.0-N50	10.28	17.24	15.44	0.60	0.67
C175×60-t2.0-N75	10.69	17.73	15.89	0.60	0.67
C175×60-t2.0-N100	10.97	18.05	16.17	0.61	0.68
C200×75-t3.0-N50	26.04	44.52	39.89	0.58	0.65
C200×75-t3.0-N75	26.50	44.65	40.01	0.59	0.66
C200×75-t3.0-N100	27.10	45.46	40.74	0.60	0.67
C225×75-t3.0-N50	26.45	43.23	38.74	0.61	0.68
C225×75-t3.0-N75	27.08	43.32	38.81	0.63	0.70
C225×75-t3.0-N100	26.09	43.46	38.94	0.60	0.67
C250×75-t3.0-N50	24.01	41.59	37.26	0.58	0.64
C250×75-t3.0-N75	24.39	41.99	37.62	0.58	0.65
C250×75-t3.0-N100	23.05	42.48	38.06	0.54	0.61
Mean value, (Pm)				0.59	0.66
Coefficient of variation, (Vp)				0.04	0.03
Reliability				0.42	0.88

To assess the reliability of the current and new design equations, a reliability analysis is conducted. As per AISI S100-16 [31], a design equation reliably is used for cold-formed steel component design when the reliability index (β) is more than 2.5. The web-bearing capacity coefficients required to perform such analysis are given in Table F1 of AISI S100-16 [31]. From Table 4, the experimental average value (Pm) and coefficient of variations (V_P) have been applied. The correcting factor (Cp), as well as the resisting factor (φ) equal to 0.85, were used as per guidelines from AISI S100-16 [31] for reliability index (β) determination. The detailed procedure and calculation guidelines have been presented in the AISI S100-16 [31] for more information.

As for reliability assessment, it is clear from Table 4 that the reliability index for SEI/ASCE-8 [25] is equal to 0.42 where it is less than the threshold of 2.5 for reliable design, indicating the SEI/ASCE-8 [25] is unreliable to use for the design of such channels. Accordingly, the reliability index for EN 1993-1-4 [26] is equal to 0.88. While it is slightly better than SEI/ASCE-8 [25], it is less than the threshold of 2.5, indicating that EN 1993-1-4 [26] is unreliable to use for the design of such channels.

Assessing the suitability of the web-bearing equations in the current design codes, the results demonstrate that the SEI/ASCE-8 [25], and EN 1993-1-4 [26] design codes for stainless steel structural components could be generally unreliable and unconservative to use for austenitic stainless steel channels under localised web bearing interior loading, and thus, may lead to very unsafe design practice. This indicates more accurate and reliable design equations are needed to be developed for the design of cold-formed austenitic stainless steel channels subject to localised web-bearing interior loading.

6. Conclusions

In this paper, web bearing capacity of cold-formed austenitic stainless steel unlipped channels subject to localised web-bearing interior loading is described. The results of 21 tests on unlipped channels with various cross-section sizes and thicknesses are presented. The tested channel sections had various web heights ranging from 100 mm to 250 mm, where the depth of the flat portion of the web over web thickness (h/t) ranged from 60.9 to 82.6 in the experimental programme. A nonlinear quasi-static Finite Element (FE) model was then developed. The FE model was validated against experimental test results and demonstrated good agreement in terms of bearing strength and failure modes which could be used for further development of design standards. In addition, to examine the accuracy and suitability of current design equations, the laboratory and numerical results were compared with the results predicted from the American specification SEI/ASCE 8:2002 [29] and European Standard EN 1993-1-4:2006 [30]. It was found that the design equations presented in the current design codes are unreliable and too unconservative to apply to cold-formed austenitic stainless steel channels, especially when compared to SEI/ASCE 8:2002 [29], as much as 41%.

References

1. Mohan, D.G.; Tomków, J.; Karganroudi, S.S. Laser Welding of UNS S33207 Hyper-Duplex Stainless Steel to 6061 Aluminum Alloy Using High Entropy Alloy as a Filler Material. *Appl. Sci.* **2022**, *12*, 2849. [CrossRef]
2. Yu, J.; Ho, H. Microstructure and Mechanical Properties of (Ti,Nb)C Ceramic-Reinforced 316L Stainless Steel Coating by Laser Cladding. *Appl. Sci.* **2022**, *12*, 6684. [CrossRef]
3. Gardner, L. Stability and design of stainless steel structures–Review and outlook. *Thin-Wall. Struct.* **2019**, *141*, 208–216. [CrossRef]
4. Baddoo, N.R. Stainless steel in construction: A review of research, applications, challenges and opportunities. *J. Constr. Steel Res.* **2008**, *64*, 1199–1206. [CrossRef]

5. Cashell, K.A.; Baddoo, N.R. Ferritic, Stainless steels in structural applications. *Thin-Wall. Struct.* **2014**, *83*, 169–181. [CrossRef]
6. Korvink, S.A.; van den Berg, G.J. Web crippling of stainless steel cold-formed beams. In Proceedings of the 12th International Specialty Conference on Cold-Formed Steel Structures, St. Louis, MO, USA, 18–19 October 1994; University of Missouri-Rolla: St. Louis, MO, USA, 1994; pp. 551–569.
7. Korvink, S.A.; van den Berg, G.J.; van der Merwe, P. Web crippling of stainless steel cold-formed beams. *J. Constr. Steel Res.* **1995**, *34*, 225–248. [CrossRef]
8. Li, H.T.; Young, B. Cold-formed ferritic stainless steel tubular structural members subjected to concentrated bearing loads. *Eng. Struct.* **2017**, *145*, 392–405. [CrossRef]
9. Cai, Y.; Young, B. Web crippling of lean duplex stainless steel tubular sections under concentrated end bearing loads. *Thin-Wall. Struct.* **2019**, *134*, 29–39. [CrossRef]
10. Cai, Y.; Young, B. Cold-formed lean duplex stainless steel tubular members under concentrated interior bearing loads. *J. Struct. Eng.* **2019**, *145*, 04019056. [CrossRef]
11. Yousefi, A.M.; Samali, B.; Yu, Y. Web bearing design of cold-formed austenitic stainless steel unlipped channels under localised interior loading. *Thin-Wall. Struct.* **2023**, *191*, 110946. [CrossRef]
12. Yousefi, A.M.; Samali, B.; Hajirasouliha, I. Experimental and numerical investigations of cold-formed austenitic stainless steel unlipped channels under bearing loads. *Thin-Wall. Struct.* **2020**, *152*, 106768. [CrossRef]
13. Yousefi, A.M.; Lim, J.B.P.; Clifton, G.C. Cold-formed ferritic stainless steel unlipped channels with web openings subjected to web crippling under interior-two-flange loading condition—Part I: Tests and finite element model validation. *Thin-Wall. Struct.* **2017**, *116*, 333–341. [CrossRef]
14. Yousefi, A.M.; Lim, J.B.P.; Clifton, G.C. Cold-formed ferritic stainless steel unlipped channels with web openings subjected to web crippling under interior-two-flange loading condition—Part II: Parametric study and design equations. *Thin-Wall. Struct.* **2017**, *116*, 342–356. [CrossRef]
15. Yousefi, A.M.; Lim, J.B.P.; Clifton, G.C. Web bearing capacity of unlipped cold-formed ferritic stainless steel channels with perforated web subject to end-two-flange (ETF) loading. *Eng. Struct.* **2017**, *152*, 804–818. [CrossRef]
16. Yousefi, A.M.; Lim, J.B.P.; Clifton, G.C. Web crippling design of cold-formed ferritic stainless steel unlipped channels with fastened flanges under end-two-flange loading. *J. Constr. Steel Res.* **2019**, *152*, 12–28. [CrossRef]
17. Yousefi, A.M.; Lim, J.B.P.; Uzzaman, A.; Lian, Y.; Clifton, G.C.; Young, B. Web crippling strength of cold-formed stainless steel lipped channel-sections with web openings subjected to Interior-One-Flange loading condition. *Steel Compos. Struct. Int. J.* **2016**, *21*, 629–659. [CrossRef]
18. Yousefi, A.M.; Lim, J.B.P.; Uzzaman, A.; Lian, Y.; Clifton, G.C.; Young, B. Design of cold-formed stainless steel lipped channel-sections with web openings subjected to web crippling under End-One-Flange loading condition. *Adv. Struct. Eng.* **2017**, *20*, 1024–1045. [CrossRef]
19. Yousefi, A.M.; Uzzaman, A.; Lim, J.B.P.; Clifton, G.C.; Young, B. Numerical investigation of web crippling strength in cold-formed stainless steel lipped channels with web openings subjected to interior-two-flange loading condition. *Steel Compos. Struct. Int. J.* **2017**, *23*, 363–383. [CrossRef]
20. Yousefi, A.M.; Uzzaman, A.; Lim, J.B.P.; Clifton, G.C.; Young, B. Web crippling strength of cold-formed stainless steel lipped channels with web perforations under end-two-flange loading. *Adv. Struct. Eng.* **2017**, *20*, 1845–1863. [CrossRef]
21. Yousefi, A.M.; Samali, B. Design of cold-formed ferritic stainless steel unlipped channels with offset web openings and unfastened flanges subject to web bearing failure under one-flange load scenarios. *Structures* **2020**, *27*, 194–211. [CrossRef]
22. Yousefi, A.M.; Lim, J.B.P.; Clifton, G.C. Cold-formed ferritic stainless steel unlipped channels with web perforations subject to web crippling under one-flange loadings. *Construct. Build. Mats.* **2018**, *191*, 713–725. [CrossRef]
23. Yousefi, A.M.; Lim, J.B.P.; Clifton, G.C. Web crippling strength of perforated cold-formed ferritic stainless steel unlipped channels with restrained flanges under one-flange loadings. *Thin-Wall. Struct.* **2019**, *137*, 94–105. [CrossRef]
24. *AS/NZS 4673:2001*; Cold-Formed Stainless Steel Structures. Australian/New Zealand Standard (AS/NZS): Sydney, Australia, 2001.
25. *SEI/ASCE 8–02*; Specification for the Design of Cold-Formed Stainless Steel Structural Members. American Society of Civil Engineers (ASCE): Reston, VA, USA, 2002.
26. European Committee for Standardization (CEN). *Eurocode 3: Design of Steel Structures—Part 1.4 (EN 1993-1-4). General Rules—Supplementary Rules for Stainless Steels*; European Committee for Standardization (CEN): Brussel, Belgium, 2006.
27. European Committee for Standardization (CEN). *Eurocode 3: Design of Steel Structures—Part 1.3 (EN 1993-1-3). General Rules—Supplementary Rules for Cold-Formed Members and Sheeting*; European Committee for Standardization (CEN): Brussel, Belgium, 2006.
28. ABAQUS Inc. *ABAQUS Analysis User's Manual*; Version 6.25; ABAQUS Inc.: Palo Alto, CA, USA, 2018.
29. *SEI/ASCE 8:2002*; Specification for the Design of Cold-Formed Stainless Steel Structural Members. ANSI: Washington, DC, USA, 2002.
30. *EN 1993-1-4:2006*; Eurocode 3—Design of Steel Structures—Part 1–4: General Rules—Supplementary Rules for Stainless Steels. iTeh, Inc.: Newark, DE, USA, 2006.
31. *AISI S100-16*; American Iron and Steel Institute Specification (AISI), North American Specification for the Design of Cold-Formed Steel Structural Members. ANSI: Washington, DC, USA, 2016.

32. Rezvani, F.H.; Yousefi, A.M.; Ronagh, H.R. Effect of span length on progressive collapse behaviour of steel moment resisting frames. *Structures* **2015**, *3*, 81–89. [CrossRef]

33. Mohammadjani, C.; Yousefi, A.M.; Cai, S.Q.; Clifton, G.C.; Lim, J.B.P. Strength and stiffness of cold-formed steel portal frame joints using quasi-static finite element analysis. *Steel Compos. Struct. Int. J.* **2017**, *25*, 727–734.

34. Natário, P.N.; Silvestre, N.; Camotim, D. Web crippling failure using quasi-static FE models. *Thin-Wall. Struct.* **2014**, *84*, 34–49. [CrossRef]

35. Yousefi, A.M.; Lim, J.B.P.; Clifton, G.C. Web crippling behaviour of unlipped cold-formed ferritic stainless steel channels subject to one-flange loading. *J. Struct. Eng.* **2018**, *144*, 04018105. [CrossRef]

36. Yousefi, A.M.; Samali, B.; Yu, Y. Shear Behaviour and design of cold-formed ferritic stainless steel channels with circular web openings. *Structures* **2021**, *33*, 4162–4175. [CrossRef]

37. Yousefi, A.M.; Samali, B.; Yu, Y. Unified design equations for web crippling failure of cold-formed ferritic stainless steel unlipped channel-sections with web holes. *J. Build. Eng.* **2022**, *45*, 103685. [CrossRef]

38. Zhang, C.; Duan, C.; Sun, L. Experimental investigation of FPS inter-storey isolation control for assembled steel structure with high aspect ratio. *Structures* **2023**, *53*, 550–567. [CrossRef]

39. Yang, Y.; Lin, B.; Zhang, W. Experimental and numerical investigation of an arch–beam joint for an arch bridge. *Arch. Civil Mech. Eng.* **2023**, *23*, 101. [CrossRef]

40. Zhai, S.Y.; Lyu, Y.F.; Cao, K.; Li, G.Q.; Wang, W.Y.; Chen, C. Seismic behavior of an innovative bolted connection with dual-slot hole for modular steel buildings. *Eng. Struct.* **2023**, *279*, 115619. [CrossRef]

41. Walport, F.; Kucukler, M.; Gardner, L. Stability design of stainless steel structures. *J. Struct. Eng.* **2022**, *148*, 04021225. [CrossRef]

42. Xing, Z.; Zhao, O.; Kucukler, M.; Gardner, L. Fire testing of austenitic stainless steel I-section beam–columns. *Thin-Walled Struct.* **2021**, *164*, 107916. [CrossRef]

43. Arrayago, I.; Real, E.; Gardner, L.; Mirambell, E. The Continuous Strength Method for the design of stainless steel hollow section beam-columns. *Eng. Struct.* **2021**, *238*, 111981. [CrossRef]

44. Dos Santos, G.B.; Gardner, L. Design recommendations for stainless steel I-sections under concentrated transverse loading. *Eng. Struct.* **2020**, *204*, 109810. [CrossRef]

45. Wang, F.; Young, B.; Gardner, L. Experimental study of square and rectangular CFDST sections with stainless steel outer tubes under axial compression. *J. Struct. Eng.* **2019**, *145*, 04019139. [CrossRef]

46. Tan, Q.H.; Gardner, L.; Han, L.H.; Song, T.Y. Fire performance of steel reinforced concrete-filled stainless steel tubular (CFSST) columns with square cross-sections. *Thin-Walled Struct.* **2019**, *143*, 106197. [CrossRef]

47. Wang, F.; Young, B.; Gardner, L. Compressive testing and numerical modelling of concrete-filled double skin CHS with austenitic stainless steel outer tubes. *Thin-Walled Struct.* **2019**, *141*, 345–359. [CrossRef]

48. Bu, Y.; Gardner, L. Local stability of laser-welded stainless steel I-sections in bending. *J. Constr. Steel Res.* **2018**, *148*, 49–64. [CrossRef]

49. Dos Santos, G.B.; Gardner, L. Testing and numerical analysis of stainless steel I-sections under concentrated end-one-flange loading. *J. Constr. Steel Res.* **2019**, *157*, 271–281. [CrossRef]

50. Yang, L.; Zhao, M.; Gardner, L.; Ning, K.; Wang, J. Member stability of stainless steel welded I-section beam-columns. *J. Constr. Steel Res.* **2019**, *155*, 33–45. [CrossRef]

51. Bu, Y.; Gardner, L. Laser-welded stainless steel I-section beam-columns: Testing, simulation and design. *Eng. Struct.* **2019**, *179*, 23–36. [CrossRef]

52. Afshan, S.; Zhao, O.; Gardner, L. Standardised material properties for numerical parametric studies of stainless steel structures and buckling curves for tubular columns. *J. Constr. Steel Res.* **2019**, *152*, 2–11. [CrossRef]

53. Cai, Y.; Zhou, F.; Wang, L.; Young, B. Design of lean duplex stainless steel tubular sections subjected to concentrated end bearing loads at elevated temperatures. *Thin-Walled Struct.* **2021**, *160*, 107298. [CrossRef]

54. Cai, Y.; Young, B. Web crippling design of lean duplex stainless steel tubular members under interior loading conditions. *Eng. Struct.* **2021**, *238*, 112192. [CrossRef]

55. Li, H.T.; Young, B. Cold-formed stainless steel RHS members undergoing combined bending and web crippling: Testing, modelling and design. *Eng. Struct.* **2022**, *250*, 113466. [CrossRef]

56. Li, H.T.; Zhan, K.J.; Young, B. Web crippling design of cold-formed high strength steel SHS and RHS at elevated temperatures. *Thin-Walled Struct.* **2022**, *180*, 109716. [CrossRef]

57. Young, B.; Ellobody, E.; He, J. Web crippling tests on cold-formed high strength steel channel sections having different stiffened flanges and stiffened web. *Thin-Walled Struct.* **2023**, *190*, 110995. [CrossRef]

58. Li, H.T.; Li, Q.Y.; Real, E.; Young, B. Web crippling resistances of cold-formed stainless steel sections: A proposal for EN 1993-1-4. *J. Constr. Steel Res.* **2023**, *210*, 108082. [CrossRef]